

CFD Calculation of Airfoil Characteristics for Performance Prediction of Vertical Axis Wind Turbine

Naoko INOUE
Kana TANAKA
Yutaka HARA
Takahiro SUMI

Department of Mechanical and Aerospace Engineering, Graduate School of Engineering
Tottori University
Koyama-Cho, Tottori, 680-8552
Japan
M11T8003C@edu.tottori-u.ac.jp

Abstract

Blade element momentum (BEM) theory is useful for the design of wind turbines because of its moderate calculation costs, but highly accurate airfoil aerodynamic data are essential in order to make reliable predictions of wind turbine performance. Such data are particularly needed for the design of vertical-axis wind turbines, which operate under a wide range of angles of attack and various Reynolds numbers. The ultimate objective of this study is to establish an aerodynamic characteristics database for various airfoils using computational fluid dynamics (CFD). This report represents the first stage of the study. Two-dimensional CFD was employed to estimate data for a symmetric airfoil for which data is already available in order to examine how accurate this method will be. The aerodynamic data obtained by CFD were employed as actual inputs for a calculation of wind turbine characteristics using BEM theory.

Key words: aerodynamic characteristics, wind turbine, CFD, BEM

1. Introduction

The topic of renewable energy has received much attention domestically and around the world, and both large and small wind turbines have been the subject of vigorous research and development as wind energy systems. Currently, 3-bladed propeller horizontal axis wind turbines are the most common type, but recently, the idea has been proposed that large floating vertical axis wind turbines (VAWTs) may provide cost savings in off-shore installations^[1]; there are also many studies of small versions of VAWTs^[2,3]. Blade element momentum (BEM) theory^[4] is useful for the design of WTs as its calculation costs are low, but highly accurate aerodynamic data are necessary in order to make very reliable predictions of WT performance^[5]. A particularly notable factor is that the angle of attack of the airfoil of a VAWT varies widely with operating conditions, and data on the variation of aerodynamic characteristics with Reynolds number (Re) must be known in order to make calculations under differing operating conditions. Most publicly available airfoil data are intended for aircraft, however; only for a quite limited set of airfoils do data include high angles of attack, up to stall (preferably, from -180° to $+180^\circ$) and a wide range of Re.

In this study, the aerodynamic forces acting on airfoils were estimated using computational fluid dynamics (CFD) for a wide range of angle of attack (α) and Re, with the ultimate goal of creating an aerodynamic characteristics database for a variety of airfoils. This report describes the first stage of this effort, in which CFD was employed on a symmetric NACA0018 section, for which previously existing data are available. An investigation was made of the range of accurate aerodynamic data that can be obtained at a relatively low calculation cost. The aerodynamic data obtained by CFD were employed as actual inputs for a calculation of WT characteristics according to the BEM theory, and these were compared with experimental results.

2. Calculation Method

2-1 Conditions for Calculation

STAR-CCM+ ver. 6.06, a general purpose CFD code, was used in this research to calculate the aerodynamic characteristics (lift coefficient C_l and drag coefficient C_d) of the airfoil. Two-dimensional steady-state

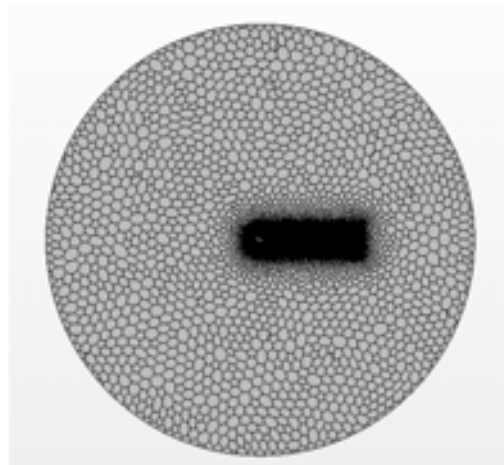
computations were carried out using a Reynolds-Averaged Navier-Stokes (RANS) model in order to minimize the computation time for each condition and to obtain results for a large number of conditions. The single-equation Spalart-Allmaras model was employed to simulate the turbulent flow model. The airfoil was a 1 m chord NACA0018 section and calculations were carried out with α values from 0° to 180° and Re values of 1.0×10^4 , 2.0×10^4 , 4.0×10^4 , 8.0×10^4 , 1.6×10^5 , 3.6×10^5 , 7.0×10^5 , 1.0×10^6 , 2.0×10^6 , 5.0×10^6 and 1.0×10^7 . The calculations were performed at 2° increments for $0^\circ \leq \alpha \leq 30^\circ$ and at 10° increments for $30^\circ \leq \alpha \leq 180^\circ$. Table 1 provides a summary of the calculation conditions.

2-2 Computational Mesh

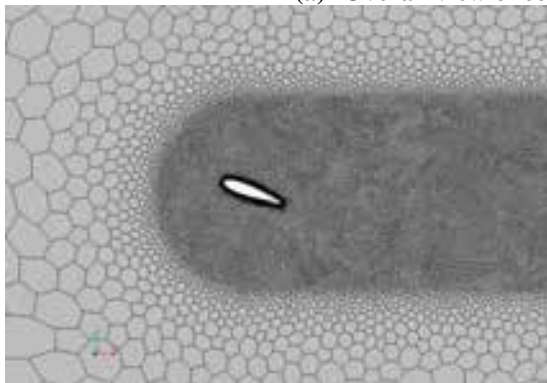
The region for these calculations was a circular volume (Region 1) whose radius was 20 times the airfoil chord (Figure 1(a)). A fine polyhedral mesh was defined near and in the wake region of the airfoil (Region 2: mesh spacing about 3% that of the far boundary; see Figure 1(b)). A prism layer mesh was employed in the vicinity of the airfoil surface (see Figure 1(c)). It was assumed that a uniform flow in the horizontal direction entered from the left far semicircle boundary of Figure 1(a) and that there was zero pressure gradient at the right far semicircle boundary. The orientation of the airfoil placed in the center of the calculation region was varied to set the value of α . Table 2 summarizes the meshing conditions.

Table 1 Conditions of calculation

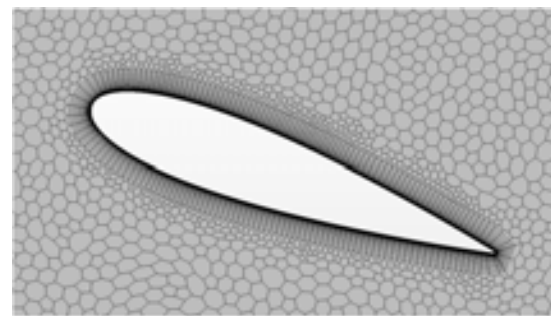
Airfoil	NACA 0018 ($c=1$ [m])
Turbulent model	Spalart-Allmaras model
Fluid	Compressible ideal gas Temperature: 293[K] (at far field)



(a) Overall view of computational domain (region1+2)



(b) Close-up view of computational mesh near region 2



(c) Close-up view of computational mesh near airfoil surface

Fig. 1 Details of computational mesh

Table 2 Conditions of computational mesh

The minimum mesh width of a surface area perpendicular direction	4×10^{-5} [m]
The range of a prism layer mesh	0.05 [m] (direction perpendicular to a field)
The number of layers of a prism layer mesh	30
The total number of nodes	About 65000
The total number of cell	About 35000

2-3 Post-processing

These calculations assumed steady state conditions even for flow fields with separation, which are unsteady by nature. In such cases, the aerodynamic coefficients do not converge, and the solutions oscillated at a constant amplitude. When no convergent solution was obtained in this study, the arithmetic mean of the final 1000 steps of the calculation with a steady oscillation amplitude was taken when a constant amplitude had been obtained a sufficient number of times and was employed for each aerodynamic coefficient at the given calculation conditions.

3. Results of Calculations and Observations

Figure 2 shows the calculated aerodynamic characteristics of the airfoil over a wide range of α ($0^\circ - 180^\circ$) at $Re = 2 \times 10^4$. Figure 3 focuses on the low- α region of $0^\circ - 30^\circ$ at the same Re . Figures 4 and 5 provide the same results with Re of 2.0×10^6 and 1.0×10^7 over the same low- α region. The solid lines in Figures 2 through 5 represent the values published in the literature for comparison. At $Re = 1.0 \times 10^4 - 1.6 \times 10^5$ and $0^\circ \leq \alpha \leq 30^\circ$, the data of Kumar *et al.*^[6] were chosen for CFD modeling of the laminar-turbulent flow transition. The data of Sheldahl *et al.*^[7], based on observed values and extrapolation of numerical values, were used for other α ranges and Re conditions.

The C_l values over the wide range of α presented in Figure 2(a) are fairly close to the values given in the literature, but the C_d values in Figure 2(b) differ significantly from the published values at around $\alpha = 90^\circ$. This was typical of the findings at all Re .

Considering Figure 3(a) and Figure 4(a), up to stall, C_l is nearly identical to the published values, but tends to be higher than those values throughout the post-stall region. The causes of this may be that the present method did not consider the laminar-turbulent flow transition, and in addition, since it was a 2-dimensional computation, it neglected the dissipation of vortices. The values of C_d are also higher than the published values throughout the α range in Figure 3(b) and in the pre-stall range in Figure 4(b).

Comparing the calculated values for C_l and C_d at the higher Re value of 1.0×10^7 (Figure 5), again, we find that they both differ significantly from the values in the literature. This suggests that the mesh in this calculation did not provide sufficient resolution.

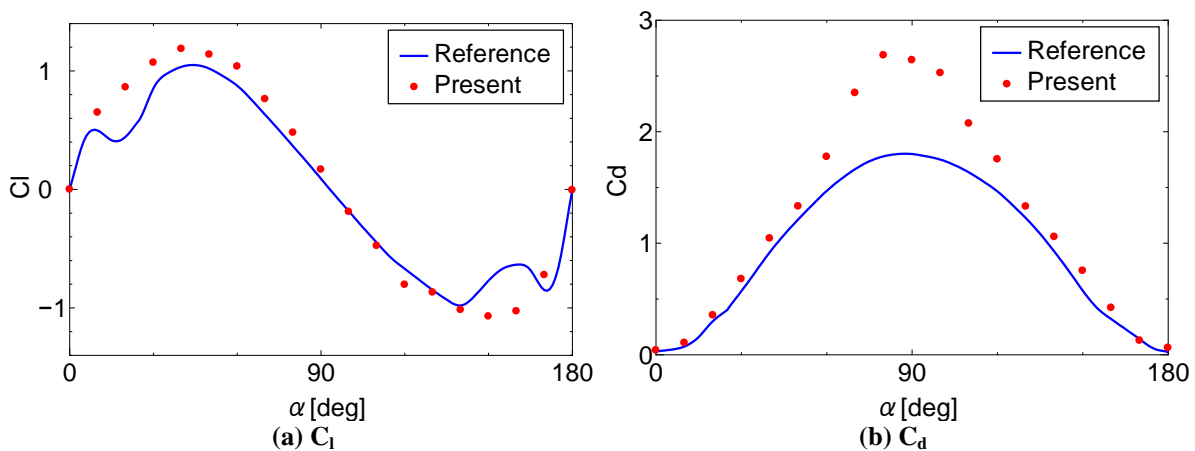


Fig. 2 Aerodynamic characteristics of airfoil ($Re=2 \times 10^4$)

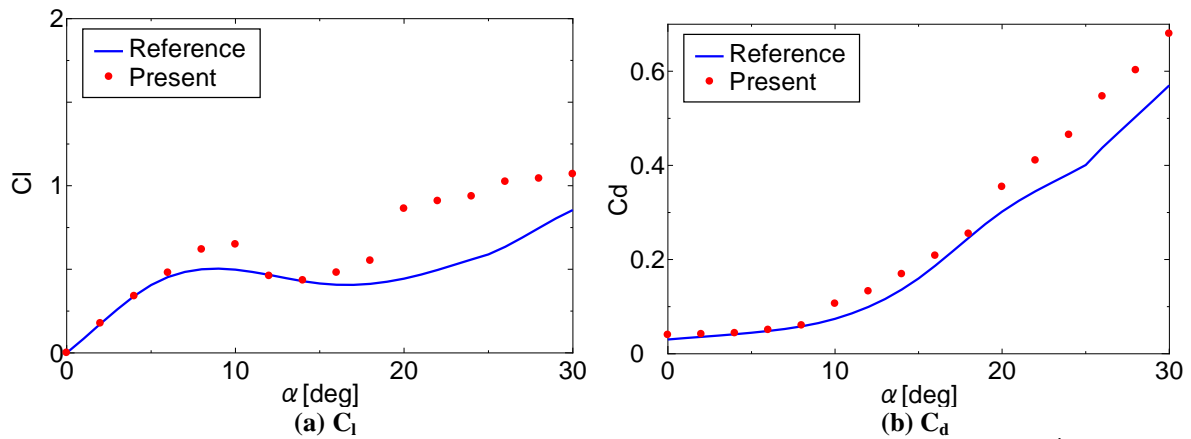


Fig. 3 Aerodynamic characteristics of airfoil in low angles of attack ($Re=2 \times 10^4$)

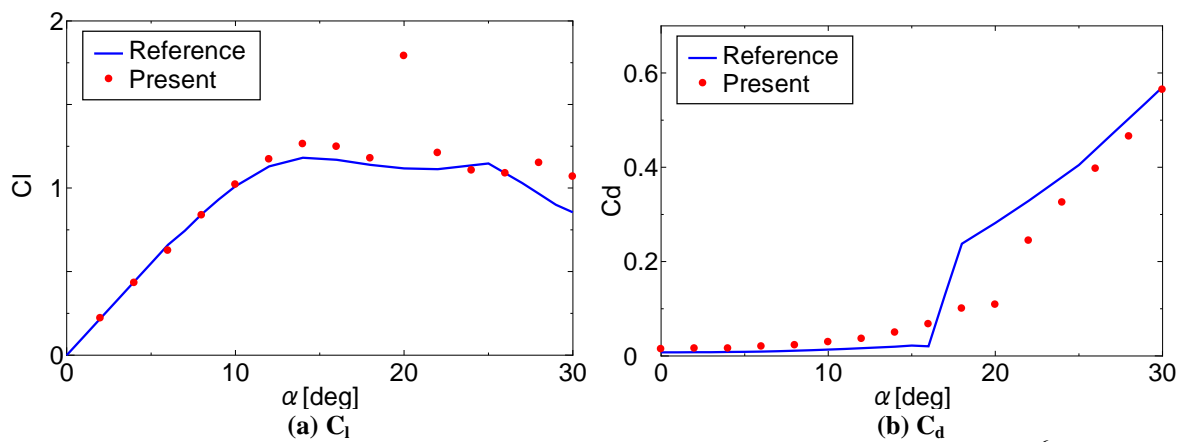


Fig. 4 Aerodynamic characteristics of airfoil in low angles of attack ($Re=2 \times 10^6$)

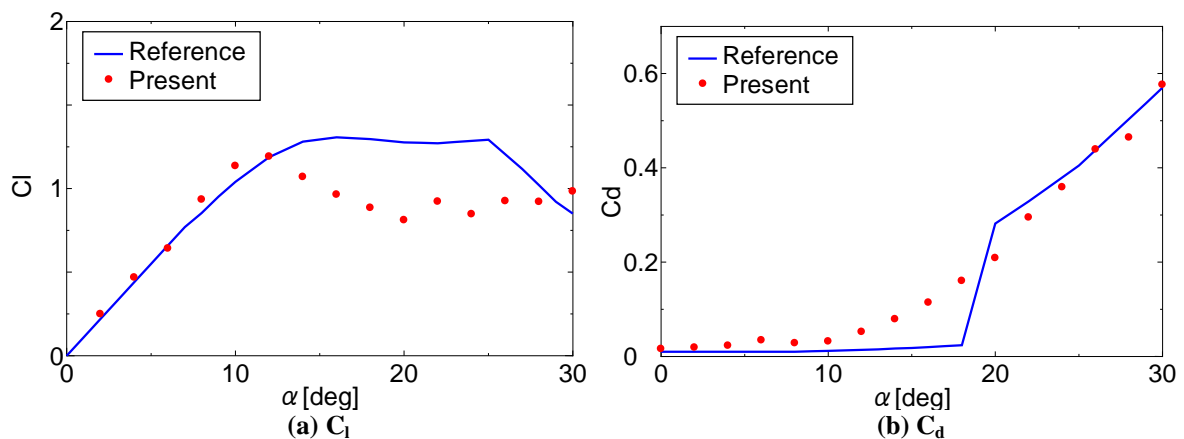


Fig. 5 Aerodynamic characteristics of airfoil in low angles of attack ($Re=1 \times 10^7$)

The aerodynamic data obtained in these calculations were converted to data at 1-degree increments using spline interpolation and those results were used to calculate the lift-drag ratio (C_l/C_d). Those ratios are provided in Figure 6 for all the specified Re (11 values) over the α range of $0^\circ - 30^\circ$. Figure 7 provides the same ratios given in the literature. We see in Figure 6 that up to $Re = 1.6 \times 10^5$, the ratios obtained in these calculations have peaks with relatively smooth slopes where C_l/C_d gradually increases with Re . At $Re = 3.6 \times 10^5$ and above, however, C_l/C_d is considerably lower than indicated in the literature (Figure 7), and the α dependence of this ratio shows unnatural “bumpiness”.

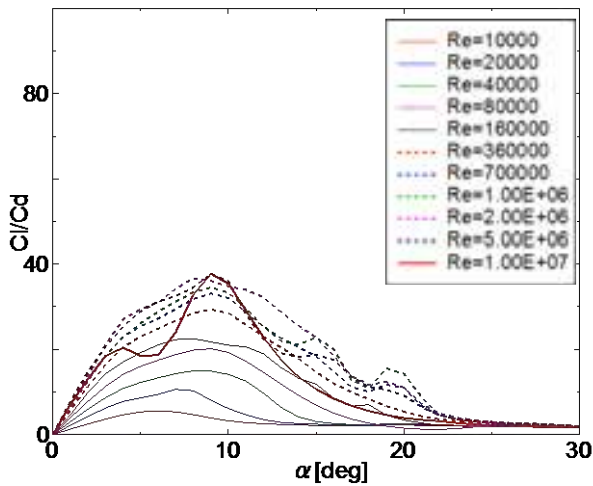


Fig. 6 The lift drag ratio obtained by the present calculation

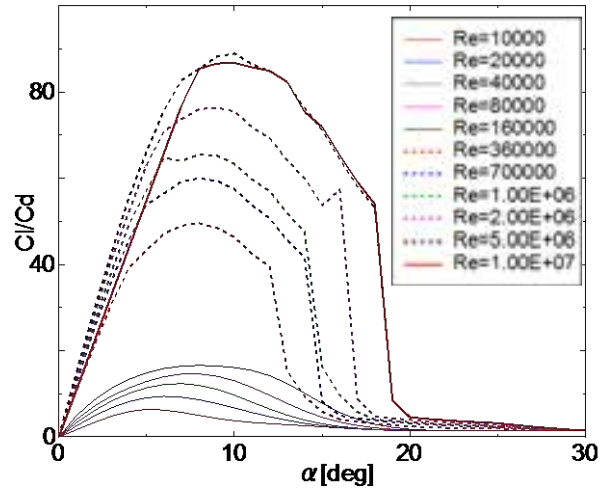


Fig. 7 The lift drag ratio obtained by the reference data [6, 7]

4. Application for Predicting Characteristics of Vertical-Axis Wind Turbine

The aerodynamic coefficients (C_l , C_d) obtained in this study were employed as the input data to estimate the performance of a VAWT using BEM theory. The double multiple streamtube theory was employed here as a flow-field model with the modified Gormont model (assuming $A_M = 1000$) to account for dynamic stall^[4]. Figure 8 presents the calculated results and experimental findings versus tip speed ratio λ for a large Darrieus wind turbine (the Sandia 17 m machine)^[8] and Figure 9 presents those for a small 0.6 m diameter experimental straight-bladed VAWT^[3]. Both graphs use the following symbology for the input data: red lines to show the present calculation results based on the aerodynamic data, pink lines for the results based on the published values of Sheldahl *et al.*, and green lines for calculations using the data of Sheldahl *et al.* partially replaced by the data of Kumar *et al.* (the solid lines in Figure 2 – Figure 5). These warn clearly that there are problems in the aerodynamic data found in this study for high Re (Figure 8); nonetheless, the results at low Re (Figure 9) tend to more closely approach the experimentally found values compared to those in the literature.

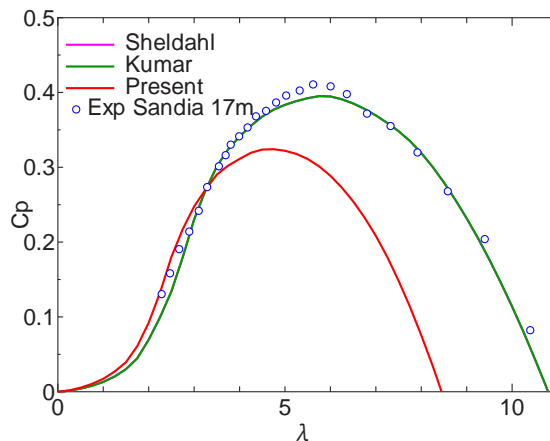


Fig. 8 Power coefficient of a large Darrieus wind turbine (SANDIA 17m , 50.6 rpm; $Re \approx 2 \times 10^6$ at $\lambda=6$)

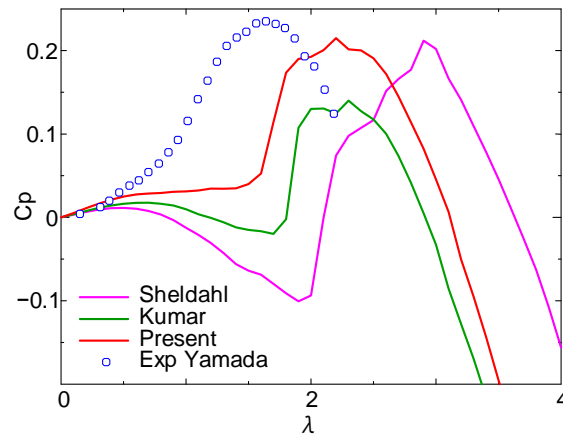


Fig. 9 Power coefficient of a micro wind turbine
(Straight-bladed VAWT, $D=0.6\text{m}$, $V=6\text{m/s}$; $\text{Re} \approx 1 \times 10^5$ at $\lambda=2$)

5. Conclusions

This study revealed that aerodynamic data for an airfoil can be calculated at relatively low cost with some degree of accuracy at low Reynolds numbers of $1.0 \times 10^4 - 1.6 \times 10^5$, in 2-dimensional steady-state computations. Nevertheless, in order to increase the accuracy under wider calculation conditions, we will examine methods for improving the mesh resolution, and incorporating unsteady calculations, 3-dimensional calculations and turbulence models.

Acknowledgements

This research was supported by a 2011 Grant-in-Aid for Scientific Research ((C)23561031) and also with aid from the Tottori University President's office, 2012 budget. We extend our deep gratitude to Seiji Yamada of the Yamaguchi Prefectural Industrial Technology Institute for providing essential wind turbine experimental data.

References

- [1] Akimoto, H., Tanaka, K., Uzawa, K., Floating axis wind turbines for offshore power generation – a conceptual study, *Environmental Research Letters*, Vol.6, No.4, (2011), 044017.
- [2] Yutaka, H., Proposal of Low Center-of-Gravity Vertical Axis Wind Turbine and Performance Prediction with Blade Element Momentum Theory, *Wind Energy*, 35-2, (2011), pp.134-139.
- [3] Yamada, S., Tamura, T., Mochizuki, S., Effects of Wing Section on Mean Characteristics and Temporal Torque Variation for a Small Straight-Bladed Vertical Axis Wind Turbine, *J. Fluid Science and Technology*, Vol.6, No.6, (2011), pp.875-886.
- [4] Paraschivoiu, I., *Wind Turbine Design with Emphasis on Darrieus Concept*, Polytechnic International Press, (2002).
- [5] Hansen, M. O. L., Madsen, H. A., Review Paper on Wind Turbine Aerodynamics, *J. Fluids Engineering*, 133-11, (2011), 114001-1.
- [6] Kumar, V., Paraschivoiu, M., Paraschivoiu, I., Low Reynolds Number Vertical Axis Wind Turbine for Mars, *Wind Engineering*, Vol.34, No.4, (2010), pp.461-476.

- [7] Sheldahl, R. E., Klimas, P. C., Aerodynamic Characteristics of Seven Symmetrical Airfoil Sections Through 180-Degree Angle of Attack for Use in Aerodynamic Analysis of Vertical Axis Wind Turbines, *Sandia Report*, (1981), SAND80-2114.
- [8] Wilson, R. E., Walker, S. N., Fixed - Wake Analysis of the Darrieus Rotor, *Sandia Report*, (1981), SAND81-7026.